

Evaluation of Temporal Complexity Reduction Techniques Applied to Storage Expansion Planning in Power System Models

Oriol Raventós^{1,*}, Julian Bartels¹

Abstract—The growing share of renewable energy results in a more challenging and computationally more demanding modelling of energy transmission systems. This is mainly due to the widely distributed weather-dependent electricity generation. This article evaluates two different methods to reduce the temporal complexity of a power grid model with extendable storage capacity. The goal of the reduction techniques is to accelerate the computation of the linear optimal power flow. The reduction is achieved by choosing a small number of representative time periods to represent one whole year. To select representative time periods, the hierarchical clustering is used to aggregate either adjacent hours or independently distributed days into clusters of time series. The efficiency of the aggregation is evaluated by means of the error of the objective value and the time reduction of the linear optimal power flow. Some statistical indicators are also introduced with the intention of anticipating the accuracy of the aggregations. Further, both the influence of the size of the network and the efficiency of parallel computation in the optimization process are analyzed. As a test case, the transmission network of the northernmost German federal state of Schleswig-Holstein with a scenario corresponding to the year 2035 is considered. The considered scenario is characterized by a high share of installed renewables and the extendability of the storage capacity.

Index Terms—Power system modelling, energy system modelling, renewable energy, linear optimal power flow, time series aggregation, storage capacity expansion planning.

I. INTRODUCTION

ONE of the most accepted key strategies to address Global Warming is the substantial increase of renewable energy capacity. This requires a significant transformation of the power network, from few stable big power plants to many weather-fluctuating widely-distributed small power sources. Therefore, in order to achieve a successful energy transition, detailed network and storage planning is required. The main objective of this article is to evaluate different *time series aggregation methods* (TSAMs) to reduce the computational time of the *linear optimal power flow* (LOPF), which is the linear approximation of the power flow equations while minimizing the total system costs. A TSAM approximates the input time series for one whole year, i.e. the load and the renewable energy generation, by a small set of representative time periods (in our case hours or days), each representing a cluster of periods. The procedure used here involves the

following steps: cluster the time series in groups of periods, choose a representative of each cluster, and adapt the corresponding equations on the linear power flow problem. The necessary tracking of the state of charge of the storage units makes the implementation of the time series clustering more challenging. Moreover, the high shares of unpredictable renewable energy sources lead to a potentially less accurate approximation of the wind energy time series.

The present contribution compares the coupled days hierarchical clustering, [1], which will be denoted here by *hierarchical clustering*, with the adjacent hours hierarchical clustering, [2], denoted here by *chronological clustering*. The comparison will be in terms of computational time and error. In [2], the chronological clustering is shown to be more efficient than other clustering methods that ignore the consistency of the state of charge. This result is expectable in a system with a large storage capacity.

To our knowledge, this is the first article which compares the chronological clustering to another method that keeps a consistent state of charge. Other clustering methods (like *k*-means), other algorithm implementations, or other types of periods (like weeks) will not be considered here, since we set the scope of this study to the two methods known to be computationally the more robust and efficient, cf. [1], [2], [3], [4], and [5]. The approaches used will be evaluated on a reference energy system developed in the *Open Electricity Grid Optimization project* (open_eGo) [6]. The problem evaluated is a linear optimization problem implemented in the open source Python package *Python for Power System Analysis* (PyPSA), [7]. In contrast to many of the publications mentioned above, which consider between 10 and 50 time series, our test case uses 437 time series generating a linear problem with up to 6 million variables and 6 million equations. In addition, this contribution compares the computational time reduction (not only the precision of the approximation) and, further, analyses the influence of the size of the network and the potential of parallel computation.

The present contribution is structured as follows. In Section II, we shortly describe the formulation of the linear problem associated with the power flow optimization. In Section III, the clustering methods are defined in detail. Section IV contains the basic information about the methods used, the test case and the indicators used to compare the time series aggregations. Section V contains the results of the optimization of the reference test case. Section VI and Section VII contain the main results of the paper, comparing the different TSAMs.

¹The authors are with the DLR-Institut für Vernetzte Energiesysteme e.V., Carl-von-Ossietzky-Str. 15, 26129, Oldenburg, Germany. *Corresponding author, e-mail: oriol.raventosmorera@dlr.de

Section VIII and Section IX study the influence of the network size and the parallel computation on the results. Finally, the conclusions are drawn in Section X.

II. LINEAR OPTIMIZATION POWER FLOW

The linear problem computing the LOPF is implemented using the free software toolbox PyPSA, [7]. Recall that the linearization of the power flow equations introduces only negligible errors when simulating transmission systems. This is true assuming that the voltage angle differences across the branches are small, the branch resistances are negligible compared to their reactance, and voltage magnitudes can be kept at nominal values. From the many equivalent formulations to compute the LOPF in PyPSA, the *Angles+Flow multi-period formulation with long term storage* will be used here. Next, we list all the equations of this formulation using the variables and parameters as defined in Table I. For a detailed formulation we refer to [11].

The objective function minimizing the total costs is:

$$\min \left[\sum_t \left(\omega_t \left(\sum_{i,s} o_{i,s} g_{i,s,t} + \sum_{i,r} o_{i,r} [h_{i,r,t}]^+ \right) + \sum_{i,s} c_{i,s} G_{i,s} + \sum_{i,r} c_{i,r} H_{i,r} \right) \right], \quad (1)$$

where, the weighting is such that $\sum_t \omega_t = 8760$. The buses power balance is defined by:

$$p_{i,t} = \sum_s g_{i,s,t} - l_{i,t} \quad \forall i \text{ and } t, \quad (2)$$

with power dispatch bounds:

$$\tilde{g}_{i,s,t} G_{i,s} \leq g_{i,s,t} \leq \bar{g}_{i,s,t} G_{i,s} \quad \forall i, s \text{ and } t. \quad (3)$$

The power flow limits are expressed by:

$$|f_{\ell,t}| \leq F_{\ell} \quad \forall \ell \text{ and } t \quad (4)$$

and the Kirchhoff current laws take the form:

$$f_{\ell,t} = \sum_{i_i} (BK^T)_t \theta_{i,t} \quad \forall \ell \text{ and } t, \quad (5)$$

$$p_{i,t} = \sum_{\ell_i} K_t f_{\ell,t} \quad \forall i \text{ and } t, \text{ and} \quad (6)$$

$$\theta_{0,t} = 0 \quad \forall t. \quad (7)$$

We also consider the following constraints:

$$\tilde{G}_{i,s} \leq G_{i,s} \leq \bar{G}_{i,s} \quad \forall i, s, \quad (8)$$

$$\tilde{h}_{i,r,t} H_{i,r} \leq h_{i,r,t} \leq \bar{h}_{i,r,t} H_{i,r} \quad \forall r, i \text{ and } t, \quad (9)$$

$$\tilde{H}_{i,r} \leq H_{i,r} \leq \bar{H}_{i,r} \quad \forall i, r, \quad (10)$$

$$0 \leq e_{i,r,t} \leq q_{i,r} H_{i,r} \quad \forall i, r \text{ and } t, \quad (11)$$

and the equations keeping track of the state of charge:

$$e_{i,r,t} = (1 - \eta_{i,r}^{loss})^{\omega_t} e_{i,r,t-1} + \omega_t \left(\eta_{i,r}^{char} [h_{i,r,t}]^+ - \frac{1}{\eta_{i,r}^{dis}} [h_{i,s,t}]^- \right) \quad \forall i, r \text{ and } t, \quad (12)$$

TABLE I
VARIABLES, COEFFICIENTS AND INDICES OF THE ANGLES+FLOW MULTI-PERIOD WITH LONG TERM STORAGE FORMULATION OF THE LOPF.

	Definition
$i \in \{1, \dots, I\}$	bus labels
$\ell \in \{1, \dots, L\}$	line labels
$s \in \{1, \dots, S\}$	generation source labels at each bus
$r \in \{1, \dots, R\}$	storage source labels at each bus
$t \in \{1, \dots, T\}$	snapshots or time steps
i_{ℓ}	labels of buses adjacent to ℓ
ℓ_i	labels of lines incident to i
ω_t	weighting of snapshot in the objective function [h]
$g_{i,s,t}$	generator dispatch [MW]
$G_{i,s}$	power capacity [MW]
$\tilde{G}_{i,s}, \bar{G}_{i,s}$	installable potential [MW]
$\tilde{g}_{i,s,t}, \bar{g}_{i,s,t}$	power availability
$o_{i,s}$	operating cost of a generation source [EUR/MWh]
$c_{i,s}$	capital cost of a generation source [EUR/MW]
$\theta_{i,t}$	voltage angle at a bus [rad]
$f_{\ell,t}$	power flow in a line [MW]
F_{ℓ}	power rating [MW]
K	$I \times L$ incidence matrix
B	diagonal $L \times L$ matrix of branch susceptances
$p_{i,t}$	total active power injection [MW]
$l_{i,t}$	load [MW]
$h_{i,r,t}$	dispatch of storage [MW]
$H_{i,r}$	power capacity [MW]
$\tilde{H}_{i,r}, \bar{H}_{i,r}$	installable potential [MW]
$\tilde{h}_{i,r,t}, \bar{h}_{i,r,t}$	power availability per unit of capacity
$o_{i,r}$	operating costs of a storage unit [EUR/MWh]
$c_{i,r}$	capital cost of a storage unit [EUR/MW]
$e_{i,r,t}$	state of charge of a storage unit [MWh]
$q_{i,r}$	hours at nominal power to fill the storage unit
$\eta_{i,r}^{loss}$	storage unit losses per hour
$\eta_{i,r}^{char}$	efficiency of charge
$\eta_{i,r}^{dis}$	efficiency of discharge

assuming a *cyclic indexing*, i.e. $e_{i,r,0} = e_{i,r,T}$.

Notice that, only Equation 12 mixes together different time periods. This means that only this equation has to be modified after the time aggregation, in order to keep it coherent.

III. TIME SERIES AGGREGATION TECHNIQUES

In this section, we describe in details the two TSAMs evaluated here.

A. Data Preprocessing

The first step of a TSAM is to normalize the different time series so that the clustering would not be affected by the different orders of magnitudes of the time series. The load is normalized with respect to the maximum load value at each grid bus, whereas the energy generation is normalized across all buses, cf. [3]. Then, the time series for the load, wind and solar energy generators at all buses are concatenated in a single time series $\{x_t\}_{t=1, \dots, 8760}$.

B. Clustering

The *hierarchical clustering* groups the original time series in daily periods $\{\bar{x}_d\}_{d=1,\dots,365}$, where $\bar{x}_d = (x_{24 \cdot (d-1)+1}, \dots, x_{24 \cdot (d-1)+24})$. After that, the hierarchical clustering (as implemented in the Python package Scikit-learn) is applied to aggregate the days in a fixed number, k , of groups. This clustering method consecutively aggregates two days with minimum deviation in their data sets $\|\bar{x}_d - \bar{x}'_d\|$, where $\|\cdot\|$ indicates the Euclidean norm. This procedure is repeated until the desired number of clusters k is reached. The hierarchical clustering is chosen since it performs better than other clustering methods in the context of TSAMs, cf. [4]. The choice of daily periods has the advantage of better approximating data with daily patterns, like the load and the solar generation, but at the price of a worst approximation of the wind generation, cf. [2]. The *chronological clustering* uses the same principle as the hierarchical clustering with the additional condition to cluster only *consecutive* hours of the original time series $\{x_t\}_{t=1,\dots,8760}$, [2].

After the clustering step, the *medoid* of each cluster is chosen as representative period, that is, the element of the cluster that is closer to the mean value of all the cluster components. Notice that, other clustering algorithms chose the *centroid* of the cluster instead, which is the mean value of all the elements in the cluster. However, in the context of TSAMs, the representative periods produce better approximations than the centroid periods since they do not discard extreme periods, cf. [4].

A visualization of the two clustering methods is shown in Figure 1 for 5 representative days (respectively 120 hours) of a wind generator. Since the chronological clustering is not forced to use daily patterns (like the hierarchical clustering), it is able to capture more accurately the abrupt changes in the wind intensity. On the other hand, the load and the solar energy are very poorly approximated by the chronological clustering when not enough representative hours are considered.

C. Data Rescaling

After the clustering, the data needs to be rescaled or normalized (to reserve the preprocessing done in Section III-A), cf. [3, Step 6].

D. Adapting the Linear Problem

The chronological method, [2], reduces the equations of the linear problem. This is achieved by using just the equations corresponding to the representative hours and defining the weighting ω_t at a representative hour t as the number of components represented by t . The hierarchical method, [1, Method M1], makes the same reduction to the representative days, but also requires to keep the equations regarding the state of charge, Equation 12, for every single hour of the year. This is done using a map of the distribution of each representative day through the year.

Notice that, the chronological clustering reduces all the time dependent variables, equalities, and inequalities from 8760 to the number of clusters k . On the other hand, the hierarchical clustering has to keep all the 8760 equations corresponding to the state of charge (and the variables involved).

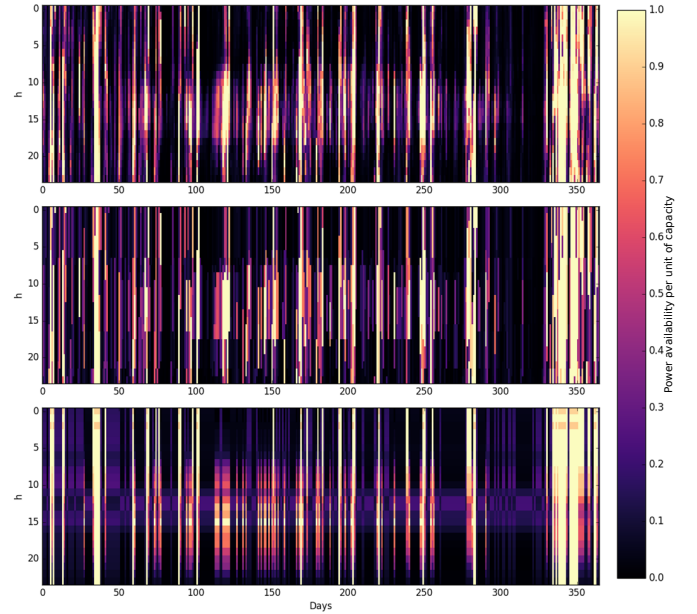


Fig. 1. Time series for a wind generator. On top the original series, in the middle the chronological clustering using 120 representative hours and at the bottom the hierarchical clustering using 5 representative days. The plots have a row for each hour of a day and a column for each day of the year.

IV. TEST CASE AND METHODS

As a test case, we use a 152 node version of the German federal state of Schleswig-Holstein power transmission network in an exogenous scenario for 2035 as described in [12]. This data is publicly available and we use it via the open source Python package eTraGo, [10] (using the grid version “0.2.11” and the scenario “SH NEP 2035”). This power network is characterized by the high availability of wind energy and the possibility of expanding the storage almost infinitely at a competitive annualized cost, i.e. it is a *storage capacity expansion planning problem*. Both the high wind availability and storage expansion option, make the system computationally more challenging to optimize. The spatial clustering of the network to 152 nodes is done using the PyPSA tool “kmeans_clustering”. A plot of the resulting network is shown in Figure 2, where the size of each bus is proportional to its installed capacity. Table II contains the global installed capacity used in the model. The main characteristics of the power grid and its components are summarized in Table III. Notice that, in the model, no capital costs are considered for generators, i.e. its installed capacity is fixed. Note also that wind and solar energy generation are assumed to have no operational costs. The properties that will most certainly influence the LOPF are the large installed capacities of wind energy (due to its unpredictable nature) and the option to extend the storage units capacity almost endlessly at a competitive (annualized) price. There are two types of storage systems considered in the model: batteries with a round-trip efficiency of 87% and a smaller power input, and the compressed hydrogen stored in underground salt caverns. This latter has a very low round-trip efficiency of 30%, but has a much bigger power input.

In a next step, PyPSA is used to formulate the linear

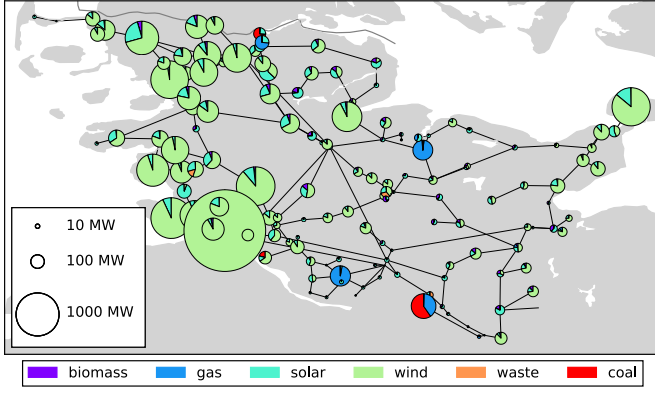


Fig. 2. Reference power grid in Schleswig-Holstein with installed capacities.

 TABLE II
INSTALLED CAPACITY BY CARRIERS [GW].

Wind	Solar	Gas	Waste	Coal	Biomass
15.56	2.57	0.68	0.05	0.27	0.5
79.17%	13.13%	3.49%	< 0.01%	1.36%	2.56%

 TABLE III
MAIN CHARACTERISTICS OF THE POWER GRID COMPONENTS.

Component	Quantity	Characteristics
Buses	152	380 kV (unified by the clustering)
Lines	132	between 182 and 3234 MVA
Snapshots	8760	
Loads	149	
Generators		fixed capacity
Biomass	125	31.4112 EUR/MWh
Gas	125	41.9344 EUR/MWh
Wind	115	0 EUR/MWh
Solar	146	0 EUR/MWh
Waste	3	39.463 EUR/MWh
Coal	3	24.7914 EUR/MWh
Storage units		extendable up to 1 TW
Batteries	149	65 822 EUR/MW, 0.01 EUR/MWh, $\eta^{loss} = 0.00694$, $\eta^{dis} = \eta^{char} = 0.9327$, $q = 6$
Hydrogen	51	65 402 EUR/MW, 0.01 EUR/MWh, $\eta^{loss} = 0.000694$, $\eta^{dis} = 0.425$, $\eta^{char} = 0.725$, $q = 168$

problem and to perform the LOPF with the Gurobi solver, [8]. Afterwards, the open source packages tsam, [9], and eTraGo, [10], were used to perform the time series aggregations and to adapt the test case network. The packages were conveniently adapted to perform the chronological clustering, the linear problem formalization from [5], and a more elaborate data pre-processing.

A. Indicators

In order to compare the LOPF of the aggregated network to the original network, we use the so called *average objective*

error (AOE), [2], which has the following general formula:

$$\left(\frac{x_{\text{aggregated}} - x_{\text{reference}}}{x_{\text{reference}}} \right) \times 100\%, \quad (13)$$

where x is the objective value in each case. We use the annual costs as objective values, which also depend on the calculated storage capacities. The same formula applied to the computational time calculates the *average time reduction* (ATR).

In order to anticipate the error in the LOPF, we define indicators based solely on the TSAMs. This is a challenging issue and there are no conclusive results in the literature, cf. [3, Section 5.1] or [17]. We will use the indicators presented in [3] together with some higher order Pearson's moment statistics detailed here under.

1) *Normalized Root Mean Square Error*: If $\{l'_{i,t}\}_{i \in I, 0 \leq t \leq 8760}$ denotes the time series at node i of the load aggregated time series, the *root mean square error* (RMSE) is defined as follows:

$$\text{RMSE}_i = \sqrt{\frac{\sum_{t=1}^T (l_{i,t} - l'_{i,t})^2}{T}}. \quad (14)$$

The *normalized* RMSE of the load, $\text{NRMSE}_{\text{load}}$, is the average of $\{\text{RMSE}_i\}$ for all $i \in I$. It is similarly defined for the time series of solar and wind energy.

As proposed in [3, Appendix B], we will also consider the RMSE of the *duration curve* of the time series, i.e. reordered in decreasing order of magnitude, which will be denoted by $\text{NRMSE}_{\text{load}}^{\text{DC}}$.

2) *Covered Variability, Skewness and Kurtosis*: The *Covered variability*, cf. [3, Equation 12], is the share of variance of the original time series represented by the aggregated one:

$$\text{VarC}_i = \frac{\sigma(l'_{i,t})}{\sigma(l_{i,t})}, \quad (15)$$

where σ is the standard deviation. We define $\text{VarC}_{\text{load}}$ as the average of $\{\text{VarC}_i\}$ for all $i \in I$. In a similar way, we define the *Covered skewness* and the *Covered kurtosis*, but using the skewness and the kurtosis instead of the standard deviation.

3) *Pearson correlation*: The Pearson correlation is defined as:

$$\text{Corr}_i = \frac{\sum_{t=1}^T (l_{i,t} - \bar{l}_i) (l'_{i,t} - \bar{l}'_i)}{\sqrt{\sum_{t=1}^T (l_{i,t} - \bar{l}_i)^2} \sqrt{\sum_{t=1}^T (l'_{i,t} - \bar{l}'_i)^2}}, \quad (16)$$

where \bar{l}_i and \bar{l}'_i are the respective mean values of the time series. The Pearson correlation of the load, $\text{Corr}_{\text{load}}$, is the average value of all Corr_i for all $i \in I$. Analogously, we define $\text{Corr}_{\text{load}}^{\text{DC}}$ for the duration curves.

B. Solver and Hardware

We use the optimization solver Gurobi with an academic licence, [8], and with the Barrier solving method (with deactivated crossover). This method was selected to enable parallel computations. We fixed the convergence tolerances to 10^{-4} . The computations were conducted on a server with 48 Intel(R) Xeon(R) Gold 6128 CPUs @ 3.40 GHz and 3 TB RAM.

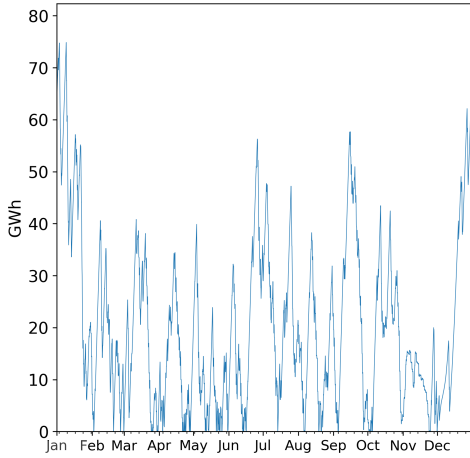


Fig. 3. Global state of charge for the non-aggregated test case.

 TABLE IV
 SHARE OF DISPATCHED ENERGY BY CARRIERS [TWh].

Wind	Solar	Gas	Waste	Coal	Biomass
9.49	1.38	0.22	0.05	0.92	1.19
71.58%	10.40%	1.65%	0.41%	6.96%	9.00%

V. TEST CASE OPTIMIZATION

The LOPF of the test case (without aggregation) results in a cost value of 103 million EUR and it is calculated in ca. 110 minutes. All the battery storage units are optimized to a capacity around 0.25 MW and 1.5 MWh and most of the compressed hydrogen underground storage caverns are around 8.7 MW and 1.5 GWh. Notice that this capacity is similar to the capacity established by other research papers for similar scenarios, cf. [13, pag. 53]. The total storage capacity of the non-aggregated test case sums up to 74.87 GWh. At the beginning of the year, the LOPF considers an almost full global state of charge (64.36 GWh), which is reasonable since there are no costs for the energy stored the previous year, see Figure 3. On the other hand, the state of charge is imposed to be the same for each storage unit at the beginning and at the end of the year.

The total share of dispatched energy carriers is shown in Table IV. The energy is highly dominated by wind energy (71.58%) and the total renewable energy share amounts to 90.98%. This is a consequence of the fact that wind energy does not have management costs, that the storage potential is very large and economically competitive, and that the wind capacity in the region of Schleswig-Holstein is meant for exportation to less windy regions (but in our model we set it only for internal consumption).

Although the load is mostly covered by wind and solar, in less windy periods there is not enough renewable energy generation to cover the energy demand, even using all the available stored energy. As an example, we plot the generated power for March stacked by carrier in Figure 4.

There is a big power curtailment of 74.11% of wind energy and of 44.33% of solar energy, which is neither used nor

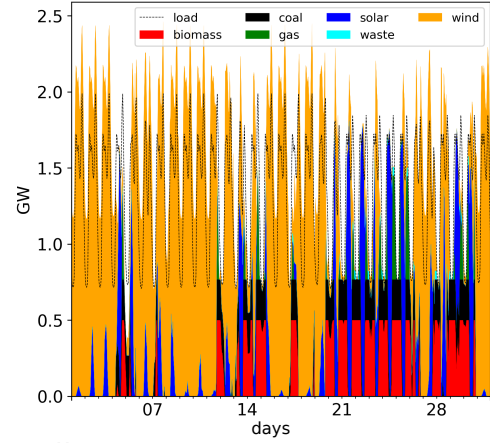


Fig. 4. Overall generated power dispatched in March stacked by carrier.

stored. This is a consequence of the fact that the installed generation capacity is fixed, but the storage is optimized in order to minimize the costs. It is also magnified by large wind generation capacity of the region. So adding the transmission lines to adjacent regions would certainly decrease the curtailment.

VI. TIME SERIES AGGREGATION EFFICIENCY

Since the various indicators from Section IV-A show the same tendencies, we show just the Pearson correlation of the duration curve as representative in Figure 5. This graphic shows more clearly how the different time series get better approximated with more representative periods. Note that the hierarchical clustering approximates the load and the solar energy better than it does for wind energy (since the latter does not show a daily pattern). The chronological clustering, on the other hand, approximates the wind energy better and it needs relatively a lot of representative hours to be able to approximate the solar energy and the load. Considered altogether, both clustering methods monotonically improve the approximation with the increase of representative periods, showing a good potential for the application that this article pursues.

VII. TIME REDUCTION AND ERROR

The average objective error (AOE) and the average time reduction (ATR) for an increasing number of representative periods for the different TSAMs are shown in Figure 6 and Figure 7. With the chronological clustering, the error is reduced almost monotonically to zero, although it is very high when we consider just few representative hours. Most notably, the computational time is reduced very significantly. For instance, with 2400 representative hours we have an AOE of less than 1% and a time reduction of 88%. Notice that, the AOE is mostly negative, meaning that the global costs of the system, i.e. the objective value, is underestimated. This means that the storage capacity needed by the system is underestimated, see Figure 8. This is probably due to the inaccurate representation of the variability of the available wind energy, which is also the most curtailed, see Figure 9.

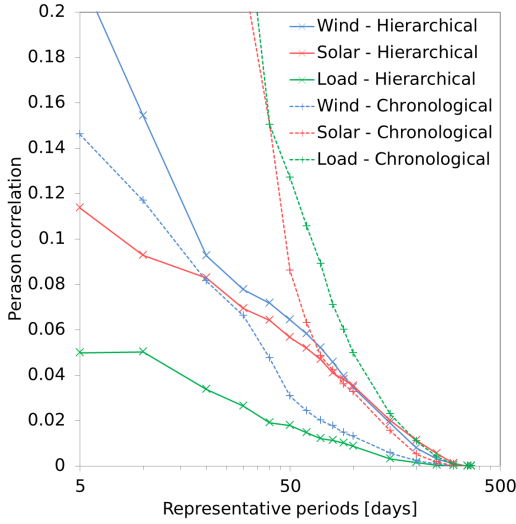


Fig. 5. Pearson correlation for the hierarchical and chronological clustering for the load, wind and solar energy, using different representative periods.

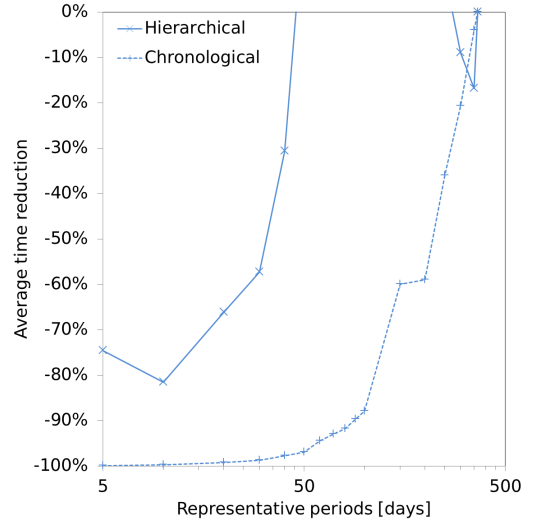


Fig. 7. Average time reduction for the hierarchical and chronological clustering using different representative periods.

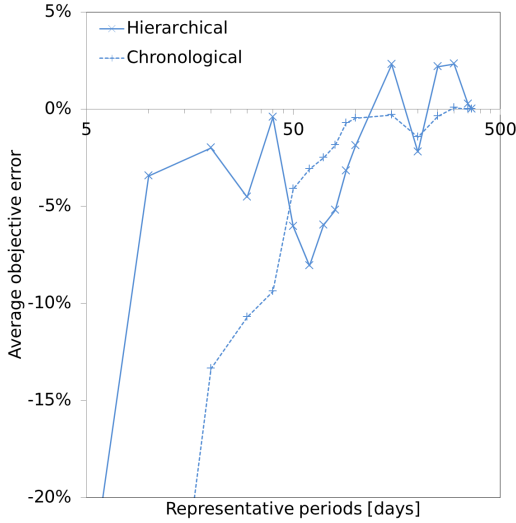


Fig. 6. Average objective error for the hierarchical and chronological clustering using different representative periods.

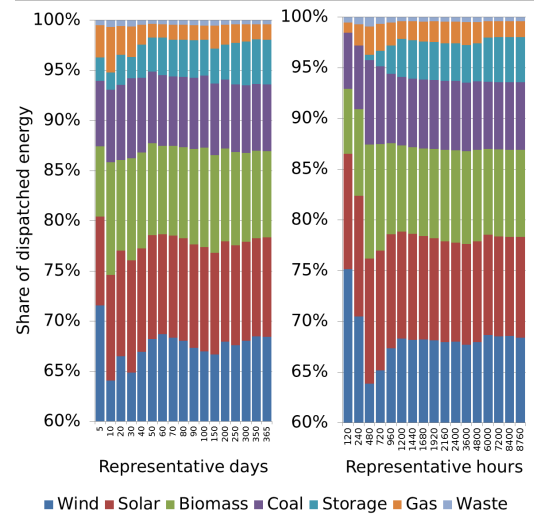


Fig. 8. Share of dispatched energy for the hierarchical method (left) and the chronological method (right). Notice that wind energy is always above the 60 % share.

On the other hand, the hierarchical clustering shows a more chaotic error convergence and the time reduction is not considerable. In fact, cases with 50 representative days or more take more time to compute than the original problem, which makes this aggregation useless. This happens because although the time aggregation creates a smaller linear problem, the equations representing the state of charge tangle the variables together in a way that interfere with the solving algorithm. Even if the AOE is very small for 40 representative days, it only reduces the computational time by 30 %. Even worse is the fact that the error does not reduces gradually nor monotonically, hence making it difficult to decide for a convenient number of representative days to use.

The chaotic behaviour of the AOE obtained for the hierarchical clustering was not mentioned in the article where the method was introduced, [1]. This may be due to the much smaller network used (see Section VIII) and that the opti-

mization is carried out using a *mixed integer linear program* (MILP). This behaviour can be, nevertheless, observed in [5, Figure 6] for an *island system* with two storage units. However, contrary to our results, in this reference, the computational time is always reduced by the hierarchical clustering. As we will see in Section VIII, this is a consequence of the fact that they use a much smaller network compared to ours. In [4], they also introduce two alternative implementations of the hierarchical clustering aimed at further reducing the computational time. However, when tested with our test case, we obtain a similar ATR (Figure 7) as for the original method formulation [1].

The results of the chronological clustering are consistent with the results in [2, Figure 3], where the method was introduced. However, in that article, it is compared to the clustering of (non-adjacent) representative days without changing the equations tracking the state of charge (Equation 12). That

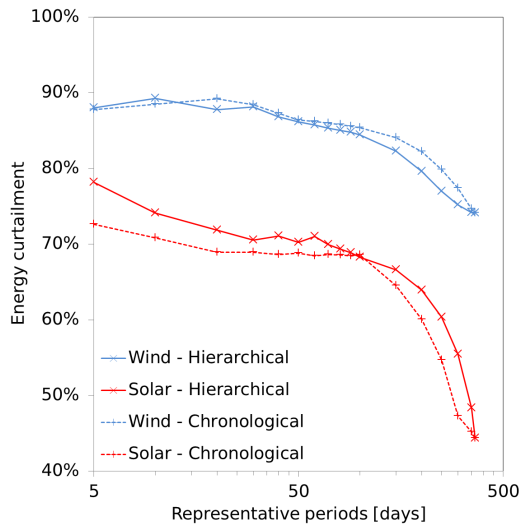


Fig. 9. Curtailment of wind and solar energy for the hierarchical and chronological clustering using different representative periods.

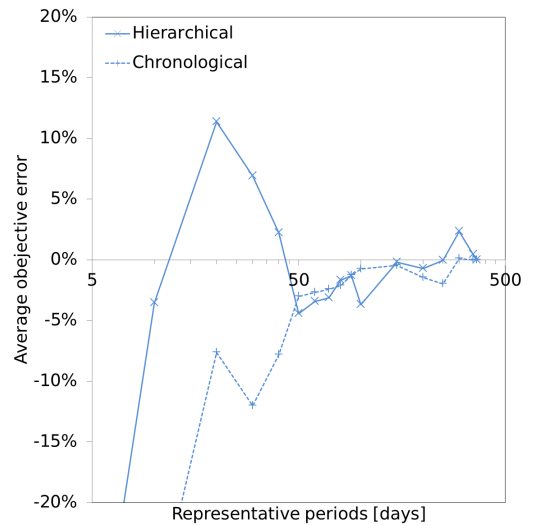


Fig. 10. Average objective error for the 10 nodes test case for the hierarchical and chronological clustering using different representative periods.

makes the error much bigger than the hierarchical method presented here (to the point of making the clustering methods useless as already observed in [4] and [1]). The advantage of the methods compared in [2] is that the computational time reduction is similar in all of them, cf. [2, Figure 4], and no anomaly (as in Figure 7) is observed. What our results show is that the hierarchical clustering can actually give very good approximations, but in an unpredictable way and not necessarily reducing the computational time.

Correlation between AOE and indicators

We studied all the possible correlations with each indicator in Section IV-A and the AOE and found no significant relation. This latter means that there is no way to detect if with a very few number of representative periods (in our case for 40 representative days) we can obtain a good approximation by just considering those indicators. Even for the chronological clustering it is difficult to predict how many representative hours can result in a small error. We can, nevertheless, infer that a good approximation of the wind energy and its variability produces a smaller error than a better approximation of the load and the solar energy. That would explain why the chronological AOE has a better behaviour.

An alternative heuristic method to decide the number of representative periods is to progressively compare the objective value of the network aggregated to k nodes with the network aggregated to $k - 1$ nodes. Nevertheless, it can only be helpful with the chronological clustering approach. In the case of the hierarchical clustering, because of its chaotic behaviour, this method does not give a good indicator of the error convergence, see Figure 6.

VIII. INFLUENCE OF THE POWER NETWORK SIZE

The results of Section VII for our test case were also confirmed by repeating the calculations for other power networks of similar or bigger size constructed from the open_eGo network, cf. [6], and the PyPSA-Eur network, cf. [14]. However,

if the size of the power network is reduced, the computational time reduction of the hierarchical clustering has a better behaviour.

In Figure 10 and Figure 11, we show the AOE and the ATR, respectively, for the test case of a power network spatially clustered to 10 nodes. As in the test case, the AOE of the hierarchical method still has a rather chaotic behaviour, whereas the chronological clustering behaves in a better way. However, in this case, the hierarchical clustering does reduce significantly the computational time, although not as much as the chronological clustering. For instance, using just 50 representative days (correspondingly 1200 hours) both algorithms have a similar AOE, but the ATR of the chronological clustering is of 96 % whereas for the hierarchical clustering it is of 74 %.

It is also interesting to stress the remarkable computational simplification of the spatial clustering. The computational time is reduced by more than 95 % and the error is just of 0.01 %. Hence, if we are not interested in the spatial distribution of the storage planning, the spatial clustering is a much more efficient method to reduce the computational time than the TSAMs, at least in the system under study with a high dependency on wind energy generation.

IX. INFLUENCE OF PARALLEL COMPUTATION

The Barrier algorithm from the Gurobi solver with the academic license allows for running parallel computations with up to 8 CPU threads. To evaluate the benefits of using parallel computation combined with the TSAMs, we repeat the previous computations from Section VII, previously done with 4 CPU threads, with 1, 2 and 8 CPU threads. However, it is also important to notice that the computational time reduction is known not to increase linearly nor indefinitely when increasing the number of threads.

The absolute computational time for the hierarchical clustering and the chronological clustering as well as the different number of CPU threads used are shown in Figure 12. For

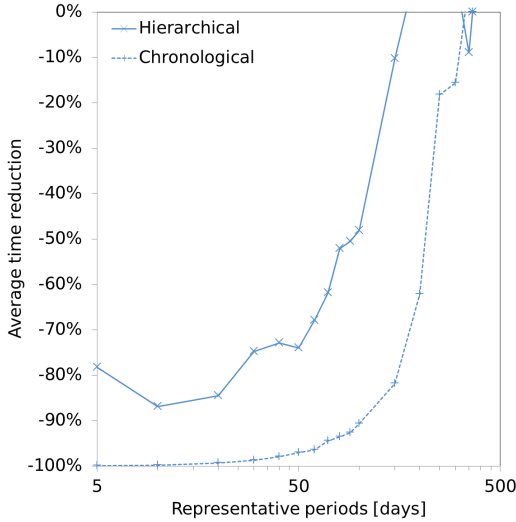


Fig. 11. Computational time for the 10 nodes test case for the hierarchical and chronological clustering using different representative periods.

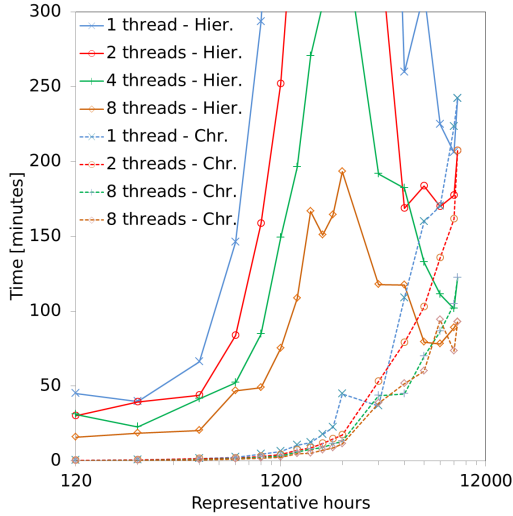


Fig. 12. Computational time for the hierarchical and chronological method using 1, 2, 4, and 8 CPU threads.

the hierarchical clustering, there is no time reduction for 5 representative days or more (like for the case of 4 CPU threads in Figure 7). For 40 days, the time reduction achieved by the parallel computation (comparing 1 thread to 8 threads) is of a similar magnitude of that of the clustering with 4 threads. On the other hand, for the chronological clustering, the advantages of parallel computation are less remarkable, since the time reduction achieved by the temporal clustering in figure 7 is bigger than the one achieved by the parallel computing.

X. CONCLUSION

This article evaluates two time series aggregation methods to reduce the computational time of the linear optimal power flow of a power grid highly dependent on wind generation and extendable storage: the hierarchical clustering of independent days and the chronological clustering of consecutive hours.

The chronological clustering gave the best results in terms of computational time reduction. Also the error obtained converges rather monotonically to zero when increasing the number of typical hours, hence having a more predictable behaviour.

The hierarchical day clustering is not always able to reduce the computational time and the error does not converges smoothly to zero, hence making it difficult to use in practice. This behaviour is expected with power networks of a similar (or bigger) size and characteristics to the test case. However, for considerably smaller networks, the hierarchical method improves considerably. The reason behind the bad performance of the hierarchical method is that the reduction of equations was cancelled out by the intertwining of the equations keeping track of the state of charge of the storage units. Furthermore, the use of more CPU threads does not contribute significantly to the computational time reduction already achieved by the TSAMs, specially with the chronological method.

A tentative correlation between different statistical indicators measuring the accuracy of the TSAMs and the error of the LOPF does not lead to clear insights. Thus, making it difficult to predict the necessary number of representative periods to guarantee a certain error of the objective value. This remains as future work.

Likewise other studies, as [15, p.20] or [16, p.11], we agree that the error of the clustering method itself is not sufficient to assess the error of the objective value.

We conclude that the choice of an appropriate clustering method depends crucially on the energy system under consideration. For the special case of an energy system highly depending on wind energy, we suggest the use of the chronological clustering using consecutive hours to simplify the time series.

ACKNOWLEDGMENT

The authors would like to thank Dr. Wided Medjroubi for suggesting the research topic in the context of the open_eGo project (BMW 0325881D) and giving continued feed back though all the research process. The authors also want to thank Jonas Hörsch, Leander Kotzur and Bruno Schyska for fruitful conversations about linear optimization of power systems. The authors acknowledge Gurobi Optimization Inc. for providing an academic licence.

REFERENCES

- [1] P. Gabrielli, M. Gazzani, E. Martelli, and M. Mazzotti, "Optimal design of multi-energy systems with seasonal storage," *Applied Energy*, vol. 219, pp. 408–424, 2018.
- [2] S. Pineda and J. M. Morales, "Chronological time-period clustering for optimal capacity expansion planning with storage," *IEEE Transactions on Power Systems*, vol. 33(6), pp. 7162–7170, 2018.
- [3] P. Nahmmacher, E. Schmid, L. Hirth, and B. Knopf, "Carpe diem: A novel approach to select representative days for long-term power system modeling," *Energy*, vol. 112, pp. 430–442, 2016.
- [4] L. Kotzur, P. Markewitz, M. Robinius, and D. Stolten, "Impact of different time series aggregation methods on optimal energy system design," *Renewable Energy*, vol. 117, pp. 474–487, 2018.
- [5] —, "Time series aggregation for energy system design: Modeling seasonal storage," *Applied Energy*, vol. 213, pp. 123–135, 2018.
- [6] "open_eGo project," <https://openegoproject.wordpress.com>.
- [7] "PyPSA github repository," <https://github.com/PyPSA/PyPSA>.

- [8] “Gurobi Optimizer,” <https://www.gurobi.com>.
- [9] “tsam github repository,” <https://github.com/FZJ-IEK3-VSA/tsam>.
- [10] “eTraGo documentation, rel. 0.7.0,” <https://etrago.readthedocs.io>.
- [11] J. Hörsch, H. Ronellenfitsch, D. Witthaut, and T. Brown, “Linear optimal power flow using cycle flows,” *Electric Power Systems Research*, vol. 158, pp. 126–135, 2018. [Online]. Available: <https://doi.org/10.1016/j.epsr.2017.12.034>
- [12] W.-D. Bunke, M. Söthe, M. Wingenbach, and C. Kaldemeyer, “(Fl)ensburg (En)ergy (S)cenarios - open_eGo Scenarios for 2014/2035/2050,” <https://osf.io/bpf36/>.
- [13] P. Elsner, B. Erlach, M. Fishedick, B. Lunz, and U. Sauer, “Flexibilitätskonzepte für die stromversorgung 2050: Technologien, szenarien, systemzusammenhänge,” acatech - Deutsche Akademie der Technikwissenschaften e. V., Tech. Rep., 2016.
- [14] “PyPSA-Eur github repository,” <https://github.com/PyPSA/pypsa-eur>.
- [15] K.-K. Cao, J. Metzendorf, and S. Birbalta, “Incorporating Power Transmission Bottlenecks into Aggregated Energy System Models,” *sustainability*, vol. 10, pp. 1916–1947, 2018.
- [16] H. Teichgraber, and A.R. Brandt, “Clustering methods to find representative periods for the optimization of energy system: An initial framework and comparison,” *Applied Energy*, vol. 239, pp. 1283–1293, 2019.
- [17] S. Fazlollahi, S. L. Bungener, P. Mandel, G. Becker, and F. Marchal, “Multi-objectives, multi-period optimization of district energy systems: I. Selection of typical operating periods,” *Computers & Chemical Engineering*, vol. 65, pp. 54–66, 2014.

Oriol Raventós received the Ph.D. in Mathematics from the University of Barcelona in 2011 and the European Master in Renewable Energy from the University of Oldenburg in 2019. He has been a postdoctoral fellow researcher in the Masaryk University in Brno and in the Regensburg University. He is currently a postdoctoral fellow at the Institute of Networked Energy Systems of the German Aerospace Center (DLR-VE) in Oldenburg, Germany. His research is mainly focused on energy system modelling and optimization.

Julian Bartels received his Master of Science in computational materials science from the University of Bremen in 2014. He has been working on electrical properties of carbon nanotubes reinforced polymers as scientific employee at the University of Bremen. Since 2017 he is working as scientific employee at the Institute of Networked Energy Systems of the German Aerospace Center (DLR-VE) in Oldenburg, Germany. His research is mainly focused on energy system modelling and optimization.